



Title	Present tectonics of the southeast of Russia as seen from GPS observations
Author(s)	Shestakov, N. V.; Gerasimenko, M. D.; Takahashi, H.; Kasahara, M.; Bormotov, V. A.; Bykov, V. G.; Kolomiets, A. G.; Gerasimov, G. N.; Vasilenko, N. F.; Prytkov, A. S.; Timofeev, V. Yu.; Ardyukov, D. G.; Kato, T.
Citation	Geophysical Journal International, 184(2), 529-540 https://doi.org/10.1111/j.1365-246X.2010.04871.x
Issue Date	2011-02
Doc URL	http://hdl.handle.net/2115/57957
Rights	This article has been accepted for publication in Geophysical Journal International ©:The Authors 2011 Published by Oxford University Press on behalf of The Royal Astronomical Society All rights reserved.
Type	article
File Information	GJI_184_529-.pdf



[Instructions for use](#)

Present tectonics of the southeast of Russia as seen from GPS observations

N. V. Shestakov,^{1,2} M. D. Gerasimenko,^{1,2} H. Takahashi,³ M. Kasahara,³ V. A. Bormotov,⁴ V. G. Bykov,⁴ A. G. Kolomiets,¹ G. N. Gerasimov,^{1,2} N. F. Vasilenko,⁵ A. S. Prytkov,⁵ V. Yu. Timofeev,⁶ D. G. Ardyukov⁶ and T. Kato⁷

¹Institute of Applied Mathematics, Far Eastern Branch of Russian Academy of Sciences, Vladivostok, Russia. E-mail: nikon@phys.dvfu.ru

²Far Eastern National University, Vladivostok, Russia

³Institute of Seismology and Volcanology, Graduate School of Science, Hokkaido University, Sapporo, Japan

⁴Institute of Tectonics and Geophysics, Far Eastern Branch of Russian Academy of Sciences, Khabarovsk, Russia

⁵Institute of Marine Geology and Geophysics, Far Eastern Branch of Russian Academy of Sciences, Yuzhno-Sakhalinsk, Russia

⁶Institute of Petroleum Geology and Geophysics, Siberian Branch of Russian Academy of Sciences, Novosibirsk, Russia

⁷Earthquake Research Institute, University of Tokyo, Tokyo, Japan

Accepted 2010 October 24. Received 2010 October 21; in original form 2009 December 13

SUMMARY

The present tectonics of Northeast Asia has been extensively investigated during the last 12 yr by using GPS techniques. Nevertheless, crustal velocity field of the southeast of Russia near the northeastern boundaries of the hypothesized Amurian microplate has not been defined yet. The GPS data collected between 1997 February and 2009 April at sites of the regional geodynamic network were used to estimate the recent geodynamic activity of this area. The calculated GPS velocities indicate almost internal (between network sites) and external (with respect to the Eurasian tectonic plate) stability of the investigated region. We have not found clear evidences of any notable present-day tectonic activity of the Central Sikhote-Alin Fault as a whole. This fault is the main tectonic unit that determines the geological structure of the investigated region. The obtained results speak in favour of the existence of a few separate blocks and a more sophisticated structure of the proposed Amurian microplate in comparison with an indivisible plate approach.

Key words: Space geodetic surveys; Plate motions; Kinematics of crustal and mantle deformation; Asia.

1 INTRODUCTION

Since the end of the last century eastern Asia has been attracting rapt attention of specialists because four tectonic plates (Eurasian—EUR, North American—NAM, Pacific—PAC and Philippine—PHI) converge (Argus & Gordon 1991; DeMets *et al.* 1994) and two independent microplates (Okhotsk—OKH and Amurian—AMU) have been hypothesized to exist here (Zonenshain & Savostin 1981; Seno *et al.* 1996). During the last 12 yr horizontal crustal velocities have been extensively investigated in this region by using GPS techniques (Kato *et al.* 1998; Heki *et al.* 1999; Takahashi *et al.* 1999; Wang *et al.* 2001; Kogan *et al.* 2000; Steblou *et al.* 2003; Calais *et al.* 2006; Meng *et al.* 2006; Jin *et al.* 2007). In spite of that, crustal velocity field of the southeast of Russia near the northeastern boundaries of the hypothesized AMU microplate has not been defined yet.

The investigated region (Fig. 1) is located quite far from a tectonic plate convergence zone controlling the present tectonics and seismicity of the Japan Island Arc, Sakhalin Island, the Kuril Island Arc and Kamchatka (Mazzotti *et al.* 2000; Gordeev *et al.* 2001;

Kato 2003; Bürgmann *et al.* 2005; Toya & Kasahara 2005 and others). According to this, the southeast of Russia is characterized by a significant deep but sparse shallow seismic activity and lack of active volcanism.

The present tectonics of the southeast of Russia is defined by a dense fault network of a complicated hierarchy (Nazarenko & Bazhanov 1987; Karsakov *et al.* 2001), which is connected with the fault system of Northeast China.

The main tectonic unit that determines the geological structure of the investigated region and strikes across it for more than 1000 kilometres from southwest to northeast is the Central Sikhote-Alin Fault (CSAF; Ivanov 1972). According to numerous geological and geophysical investigations it is a deep left-lateral strike-slip fault penetrating into the Earth's crust about 40 km (Argentov *et al.* 1976). The beginning of its formation refers to the Early Mesozoic, but the most significant relative displacements along the fault trace occurred in the Late Cretaceous. The total relative slip amplitude of the eastern CSAF flank with respect to the western one is evaluated to be 200 km in the north and 60 km in the south of the fault trace (Ivanov 1972). The information on the recent geodynamic activity

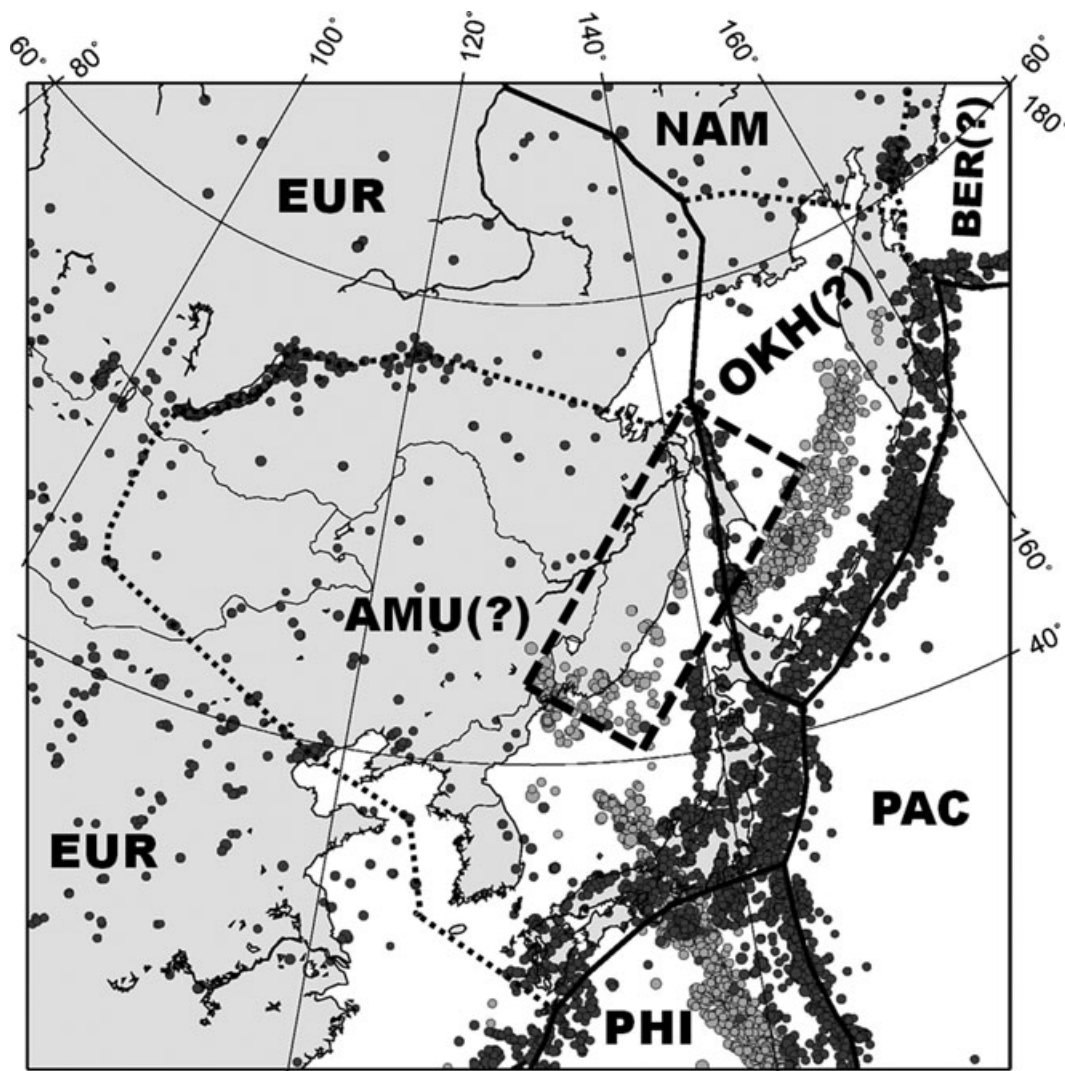


Figure 1. Tectonic sketch-map of Northeast Asia. Eurasian (EUR), North American (NAM), Pacific (PAC) and Philippine (PHI) plate boundaries are taken from NUVEL 1A model (DeMets *et al.* 1994). The hypothesized Amurian (AMU) and Okhotsk (OKH) microplate boundaries are marked by dotted line according to Wei & Seno (1998) and Seno *et al.* (1996). Seismicity is shown for a period of 1973–2009 according to USGS NEIC catalog (<http://neic.usgs.gov/neis/epic/epic.html>). The seismic events with magnitude $M \geq 4$ and depth of $H \leq 30$ km (dark grey circles) and $H \geq 300$ km (light grey circles) are represented. A dashed rectangle shows the investigated area.

of the CSAF is scanty and incomplete. Nevertheless, based on the previous geological studies, Ivanov (1972) estimated the slip-rate of the eastern CSAF flank to be equal to $5\text{--}7 \text{ mm yr}^{-1}$ with respect to the western flank. Timofeev *et al.* (2008) have recently estimated this value to be approximately equal to 1.5 mm yr^{-1} based on a velocity set of 6 GPS stations across the CSAF trace observed in campaign mode.

The main objectives of this study are: (1) to determine the crustal velocity field of the southeast of Russia based on the developed regional GPS network data, (2) to estimate the recent geodynamic activity of the CSAF as a whole, and (3) to test the correspondence of the obtained velocity field to the concept of the AMU/EUR rigid rotation.

2 GPS DATA AND ANALYSIS

The GPS data collected between 1997 February and 2009 April were involved in the analysis presented in this paper. The GPS measurement data of three types were processed: continuous, semi-

continuous (2–6 month observations during a year) and campaign-mode, which stem from the following five sources:

- (1) semi-continuous and continuous GPS measurements carried out in the southeast of Russia under collaboration of the Russian Academy of Sciences (RAS) and Association of Japanese Universities;
- (2) campaign-mode measurements conducted during 2003–2007 across the CSAF by the united team of the Institute of Tectonics and Geophysics of the Far Eastern Branch of the RAS and the Institute of Petroleum Geology and Geophysics of the Siberian Branch of the RAS (Timofeev *et al.* 2008);
- (3) continuous observations started at the GPS station VLAD in 1996 under the WING project (Kato *et al.* 1998);
- (4) continuous GPS measurements performed in the north (OKHA) and campaign-mode observations in the west (UGLG) of Sakhalin Island (Steblov *et al.* 2003; Kogan *et al.* 2003);
- (5) continuous observations conducted at the IGS (International GNSS service) stations (KHAJ, YSSK, BJFS, DAEJ (TAEJ), IRKT,

MAG0, PETP, SHAO, TSKB, USUD). The main characteristics of GPS sites located in the study area and aimed to investigate the present tectonics of the southeast of Russia are given in Table 1. It should be pointed out that the geodynamic GPS network used in this study does not uniformly cover the investigated region due to impeded access and sparse density of the population in this territory.

The GPS data were processed by using the *BERNESE Ver. 5.0 software*. At the first step, we processed GPS measurement data of our regional geodynamic GPS network together with the above mentioned IGS station data to produce daily normal equations (NEQ-files) comprising station positions and their variance-covariance terms, estimates of atmosphere-parameters, etc. (Beutler *et al.* 2007). At this processing stage only loose constraints were imposed on the GPS station positions. At the second step, all daily NEQ-files for the whole observation period were combined through the Sequential Least-Squares Estimation procedure in ADDNEQ2-module (Brockmann 1997) to produce the combined network solution and make its comparison with each daily solution for outlier detection and a search of site position shifts due to GPS antenna manipulations. After outlier removal and shift corrections all the site velocities were estimated in ADDNEQ2 without any constraints (free velocity solution). Fig. 2 shows the examples of daily repeatability of horizontal position components for continuous, semi-continuous and campaign-mode GPS sites with respect to combined solution (detrended position time series).

For estimation of the velocity component errors the model given in (Geirsson *et al.* 2006) and based on equation $\sigma_{vel} = \sigma/T$ was adopted. In this formula, σ is the weighted RMS value (WRMS) of the coordinate component residuals estimated by ADDNEQ2 after comparison of each daily solution with combined solution and T is the length of time series in years.

At the final processing step, to have our station velocities in a well-defined reference frame we transformed our free velocity solution into ITRF2008 (http://itrf.ensg.ign.fr/ITRF_solutions/2008/). This was performed through 6-parameter (3 translations and 3 rotations) Helmert transformation by minimizing differences between our free regional network and ITRF global solutions in a set of 7 common sites. The obtained ITRF2008-velocities of our network sites are summarized in Table 2.

To refer all the analyzed velocities to the stable EUR we subtracted the EUR rigid rotation from our ITRF2008-velocities. To do this, we estimated the EUR absolute rotation pole parameters by using ITRF-velocities for a set of 13 plate-defining GPS sites distributed inside the EUR stable interiors (Fig. 3). As can be seen from Fig. 3, our EUR-fixed reference frame is quite stable. All velocity residuals at the plate-defining sites are less than 1.5 mm yr⁻¹ and mostly do not exceed 1.0 mm yr⁻¹. The obtained EUR absolute rotation pole parameters ($54.2 \pm 0.7^\circ\text{N}$, $-100.7 \pm 0.5^\circ\text{E}$, $0.251 \pm 0.002^\circ$ per Myr, WRMS = 0.54 mm yr⁻¹) are quite similar to those obtained by (Wang *et al.* 2001; Altamimi *et al.* 2002; Prawirodirdjo & Bock 2004; Meng *et al.* 2006) but are considerably different from NUVEL-1A estimate (DeMets *et al.* 1994) and the values given in (Calais *et al.* 2003; Altamimi *et al.* 2007). The difference between our EUR-pole solution and those published can be mainly explained by different number and distribution of the plate-defining GPS sites. The EUR-velocities of our network sites are summarized in Table 2.

To access the local-scale crustal movements in the study area we also referred our GPS velocities to the VLAD site which has the longest continuous observation history in our GPS network and is almost stable with respect to EUR ($V_n = 0.2 \pm 0.2$, $V_e = 0.4 \pm$

0.2 mm yr^{-1}). This was performed by subtracting the EUR-velocity of the VLAD site from velocities of other network sites. The obtained velocities are close to those referred to EUR due to small magnitude of the VLAD site EUR-velocity.

3 RESULTS AND DISCUSSION

3.1 GPS velocity field

In the present study, most of the GPS site EUR-velocities obtained for the continental part of the southeast of Russia are oriented northeast with slight domination of the east component (Fig. 4). Their magnitudes are relatively small and generally do not exceed 3–4 mm yr⁻¹. The 1-sigma velocity uncertainties range from 0.2 to 1.1 mm yr⁻¹. However, two stations of our continental GPS network show the significantly different behaviour. The station ROSH is moving eastward with a magnitude of 5.7 mm yr⁻¹ which is much faster than velocities of the neighbour GPS sites EAST, MALI and BURS located 7, 64 and 70 km from ROSH (see Fig. 4). The geodetic monument of this site was installed on the roof of the brick-constructed building (see Table 1). According to this, the observed ROSH velocity is not most likely to reflect regional tectonic deformations. It is rather related to the local systematic crustal deformations or attributed to instability of the building basement. Another station SPSK has been moving nearly to the west with a magnitude of 3.6 mm yr⁻¹, which is different from movements of other continental sites. At the present stage, it is difficult to decide whether this result can be related to the present-day tectonic activity near Lake Khanka which is characterized by rare shallow seismic events (Oleynikov & Oleynikov 2006) or to some other reasons, for example, short observation period (2-yr semi-continuous measurements), some local deformations, etc. The ROSH and SPSK site velocities have been eliminated from further analysis.

Thus, the obtained velocity field for the continental part of the southeast of Russia referred to EUR speaks in favour of low-scale recent geodynamic activity and a small eastward movement (almost stability) of this region with respect to EUR. This conclusion is in a quite good agreement with the recent estimates of modern tectonics of Northeast Asia and North China, which are also characterized by small northeast and southeast velocities (England & Molnar 2005; Calais *et al.* 2006; Meng *et al.* 2006; Jin *et al.* 2007).

In contrast to the continental stations, the GPS sites located in Sakhalin Island show a coherent westward movement with velocities of 3–8 mm yr⁻¹ with respect to EUR (Fig. 4). This result indicates the existence of the GPS velocity orientation boundary between the mainland and Sakhalin. The obtained fact can explain stress accumulation and rare shallow seismic events near the western coast of Sakhalin Island and can also testify to attributability of Sakhalin to another tectonic plate (NAM or OKH). The estimated velocity magnitudes are closer to those obtained by Steblov *et al.* (2003) and Kogan & Steblov (2008), rather than to those predicted by the AMU and OKH plate models proposed by Apel *et al.* (2006). However, Sakhalin can be clearly attributed to the NAM or OKH plate only after densification of the presently operating sparse regional GPS network.

3.2 Recent geodynamic activity of the CSAF

Based on the obtained velocity field it is important to consider the following question: can the velocities estimated for the continental

Table 1. Description of the GPS network sites. Monumentation codes: RCP, reinforced concrete pillar; SSP, stainless steel pillar; SSM, stainless steel mark; SC, steel triangular or rectangular construction. Station codes: CS, continuous; SCS, semi-continuous; SMS, survey-mode site.

Site	Lon. deg.	Lat. deg.	Monumentation type	Receiver type	Antenna type	Observation period, years	Station code
KHAJ	135.046	48.521	Pillar on the roof of the brick-constructed building	ASH Z-18 JPS LEGACY TPS E_GGD	ASH701073.3 JPSREGANT_SD_E JPSREGANT_SD_E	1998.85–2000.05 2001.88–2007.83 2007.83–2009.26	CS (IGS)
YSSK	142.717	47.030	RCP on the roof of the reinforced concrete building	ASH Z-XII3 ASH Z-XII3	ASH701933B_M ASH701933B_M DOME	1999.58–2003.50 2003.50–2009.26	CS (IGS)
VLAD	131.926	43.197	SSP on the roof of the reinforced concrete building	TRM 4000SSE	TRM22020.00+GP	1997.09–2009.26	CS (WING)
GEOO	135.052	48.473	SSM on the roof of the brick-constructed building	ASH Z-XII3	ASH700718A	2004.77–2009.26	CS
OKHA	142.946	53.602	SSM on the roof of the reinforced concrete building	ASH Z-XII3	ASH700718A	1995.56–2004.80	SCS
NKHD	132.891	42.828	SSP on the roof of the brick-constructed building	ASH Z-XII3 TRM 5700	ASH700718A TRM22020.00+GP	2001.88–2003.99 2005.29–2008.98	Up to 2003.99 was SCS Since 2005.29 has been CS
ARTM	132.196	43.360	RCP on the roof of the brick-constructed building	TPS EUROCARD TPS E_GGD TPS EUROCARD TPS E_GGD TPS E_GGD	JPSREGANT_SD_E TPSCR3_GGD JPSREGANT_SD_E TPSCR3_GGD JPSREGANT_SD_E	2002.54–2004.21 2004.44–2004.47 2004.56–2004.84 2005.72–2005.88 2008.30–2008.94	Up to 2005.88 was SCS Since 2008.30 has been CS
GRNT	132.166	43.698	SC deepened into sediments	ASH Z-XII3	ASH700718A	2002.37–2005.72	SCS
ROSH	134.893	45.898	SSP on the roof of the brick-constructed building	ASH Z-XII3	ASH700718A	2002.03–2006.42	SCS
SMHK	135.818	44.346	SC deepened into sediments	ASH Z-XII3 TRM NETR5	ASH700718A TRM55971.00	2003.79–2008.80 2008.80–2009.26	SCS
TERN	136.601	45.062	SC deepened into sediments	ASH Z-XII3 TRM NETR5	ASH700718A TRM55971.00	2004.31–2008.80 2008.80–2009.26	Up to 2008.80 was SCS Since 2008.80 has been CS
SPSK	132.809	44.592	SSM on the roof of the reinforced concrete building	TPS LEGACY	TPSPG_A1	2007.24–2009.26	SCS
ZMEY	135.590	48.100	RCP deepened into sediments	TRM 4700	TRM33429.00+GP	2003.75–2007.74	SMS
GOBL	138.254	49.217	SSM deepened into bedrock	ASH Z-XII3	ASH700718A	2004.78–2007.78	SMS
MALI	134.080	45.810	SSM deepened into bedrock	TRM 4700	TRM33429.00+GP	2003.76–2006.73	SMS
EAST	135.060	46.000	SSM deepened into bedrock	TRM 4700	TRM33429.00+GP	2003.78–2006.76	SMS
BURS	135.440	45.400	SSM deepened into bedrock	TRM 4700	TRM33429.00+GP	2003.77–2006.75	SMS
NEBO	135.820	45.110	SSM deepened into bedrock	TRM 4700	TRM33429.00+GP	2003.77–2006.74	SMS
PLST	136.310	44.730	SSM deepened into bedrock	TRM 4700	TRM33429.00+GP	2004.75–2006.74	SMS
UGLG	142.065	49.076	RCP deepened into sediments	ASH Z-XII3 ASH Z-XII3	ASH700718A ASH701933B_M	1997.37–2000.19 2000.78–2003.52	SMS
VANI	139.641	49.079	SSM deepened into bedrock	ASH Z-XII3	ASH700718A	2004.78–2007.79	SMS
LID6	136.995	49.484	SSM deepened into bedrock	ASH Z-XII3	ASH700718A	2004.74–2007.70	SMS

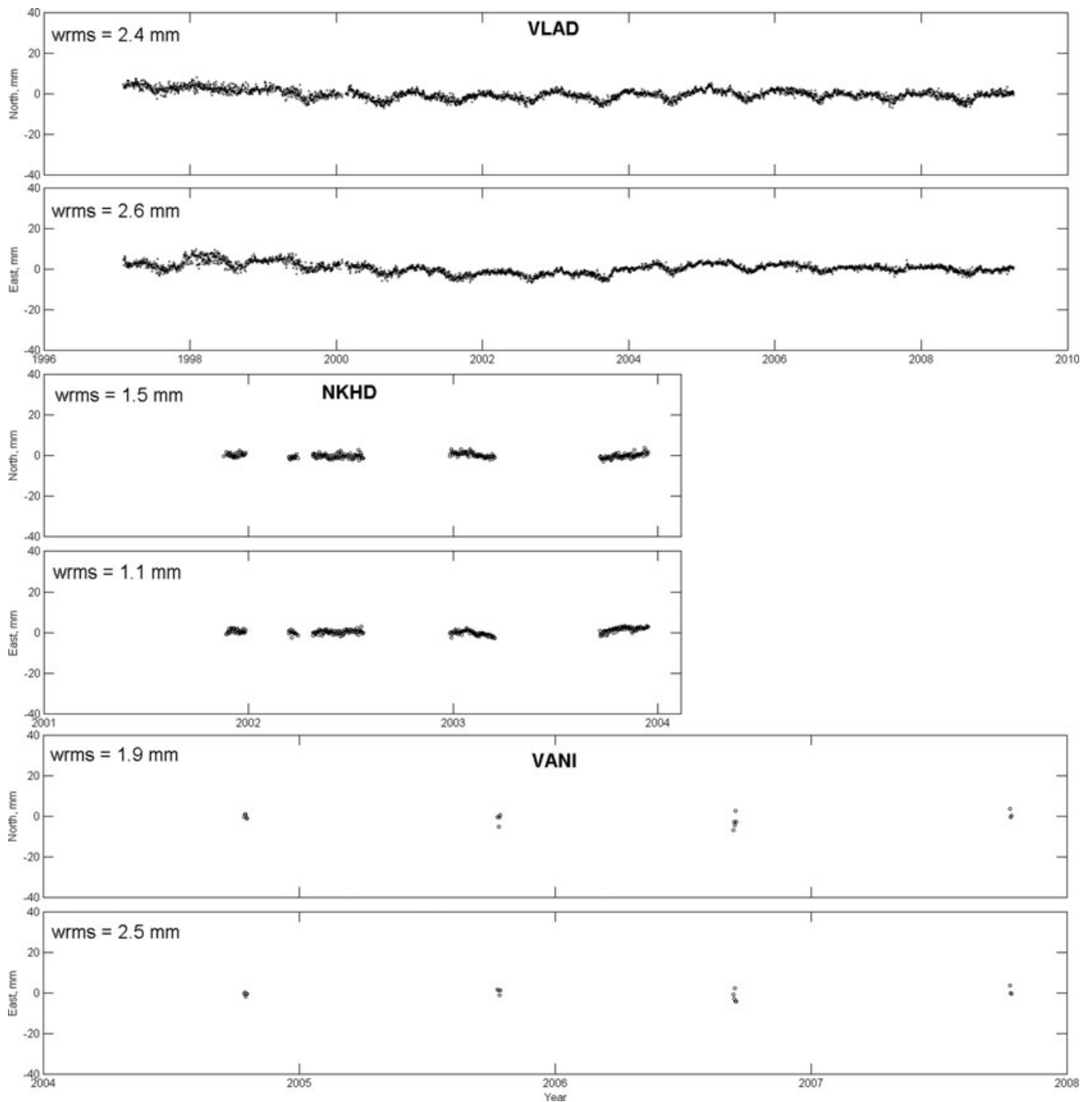


Figure 2. The examples of daily repeatability of horizontal position components for continuous, semi-continuous and campaign-mode GPS sites with respect to combined solution (detrended position time series) are shown. Outliers and shifts due to GPS antenna manipulations are removed. WRMS is the weighted RMS value of the coordinate component residuals estimated by ADDNEQ2 after comparison of each daily solution with combined solution.

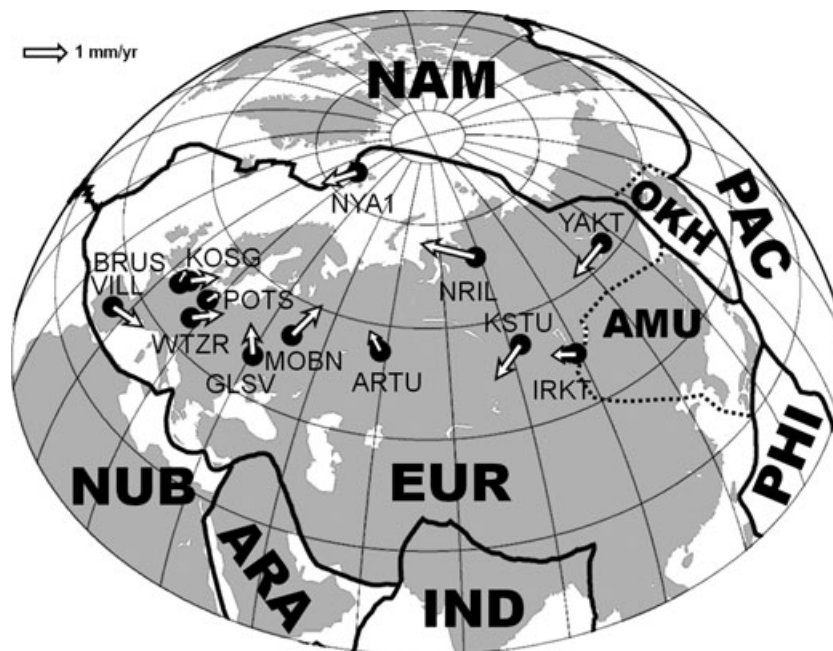
part of the southeast of Russia be associated with the recent geodynamic activity of the CSAF? To cope with this problem, we used the GPS site velocities referred to VLAD for testing three simple CSAF models: (1) zero-velocity field, that is, there are no relative movements between the eastern and western flanks of the CSAF; (2) a two-rigid-block model, that is, the eastern flank is moving as a rigid block with respect to the western flank along the CSAF trace with a constant velocity V ; (3) an ideal left-lateral strike-slip locked fault (Lisowski *et al.* 1991). The last model is determined by two parameters, H and V_H , where H is the locking depth of the fault and V_H is the tectonic block uniform slipping velocity below

the locking depth. At the present stage, it is impossible to produce more complicated and rigorous CSAF models due to low and non-uniform density of our GPS network. Totally, velocities of 16 GPS sites were used for modelling except for the velocity of the reference site VLAD.

We characterized the misfit between the model-calculated and the observed velocities in terms of χ^2/df (Stein & Gordon 1984), where df is the number of degrees of freedom for an appropriate CSAF model. A value of χ^2/df for model 1 is equal to 9.8 ($df = 16$). For model 2, we varied a value of V to minimize the misfit between the model-calculated and the observed velocities. The

Table 2. Station velocities and their 1-sigma uncertainties in ITRF2008 reference frame and with respect to EUR.

Site	Longitude deg.	Latitude deg.	ITRF2008		EUR-velocities		σ_{V_e} mm yr ⁻¹	σ_{V_n} mm yr ⁻¹
			V_e mm yr ⁻¹	V_n mm yr ⁻¹	V_e mm yr ⁻¹	V_n mm yr ⁻¹		
KHAJ	135.046	48.521	22.8	-13.8	0.9	-0.3	0.2	0.2
GEOO	135.052	48.473	23.8	-12.8	1.9	0.7	0.4	0.5
GOBL	138.254	49.217	24.0	-11.1	2.8	2.8	0.7	1.0
VANI	139.641	49.079	23.1	-14.2	2.2	0.0	0.8	0.6
LID6	136.995	49.484	23.2	-12.1	1.8	1.7	0.4	1.1
VLAD	131.926	43.197	23.7	-12.8	0.4	0.2	0.2	0.2
NKHD	132.891	42.828	23.2	-13.0	0.0	0.1	0.2	0.2
GRNT	132.166	43.698	25.4	-10.6	2.2	2.4	0.6	1.1
ROSH	134.893	45.898	27.9	-12.0	5.5	1.5	0.6	0.5
SMHK	135.818	44.346	22.5	-12.7	0.0	0.9	1.1	0.4
TERN	136.601	45.062	23.4	-11.2	1.2	2.5	0.4	0.9
ARTM	132.196	43.360	25.8	-13.0	2.6	0.0	0.3	0.3
SPSK	132.809	44.592	19.4	-13.1	-3.6	0.0	0.7	0.8
ZMEY	135.590	48.100	23.0	-13.0	1.1	0.6	0.4	0.4
MALI	134.080	45.810	24.9	-10.6	2.4	2.8	0.6	0.6
EAST	135.060	46.000	22.4	-13.1	0.0	0.4	0.5	1.0
BURS	135.440	45.400	23.1	-13.3	0.7	0.3	0.8	0.7
NEBO	135.820	45.110	24.0	-10.0	1.6	3.6	0.7	0.8
PLST	136.310	44.730	23.6	-12.8	1.2	0.9	1.0	0.9
UGLG	142.065	49.076	17.8	-13.3	-2.7	1.2	0.4	0.5
OKHA	142.946	53.602	15.5	-15.1	-3.8	-0.5	0.5	0.6
YSSK	142.717	47.030	12.6	-13.0	-8.2	1.6	0.3	0.4

**Figure 3.** Velocity residuals at the EUR plate-defining sites (the observed velocities minus calculated ones by using the absolute EUR rotation pole).

optimal V and χ^2/df values are equal to 1.4 mm yr⁻¹ and 8.7 ($df = 15$), accordingly. We also varied parameters of model 3 to minimize a χ^2/df value. The optimal value of V_H lies within the range 1.8 mm yr⁻¹ for $H = 40$ km to 1.5 mm yr⁻¹ for $H = 5$ km. The corresponding minimal misfit value is almost the same for all the parameter sets and ranges from 9.2 to 9.3 ($df = 14$).

According to the obtained misfit values there is no significant difference between the calculated χ^2/df -values for all the models. It is obvious that the reduction of χ^2/df -value for models 2 and 3 can be explained simply by introduction of the additional model

parameters. Moreover, the magnitudes of the model velocities calculated from the last two models are almost the same and do not significantly exceed errors of their observed values (Fig. 5). Thus, we can conclude that all the models approximately equally fit the observed GPS velocity field. They do not give evidence of any significant recent geodynamic activity of the CSAF as a whole, as reported by Ivanov (1972) based on geological data and Timofeev *et al.* (2008) resting upon data from a single GPS profile across the CSAF. However, the tested CSAF models do not correspond well to the observed GPS velocity field. Therefore, we cannot exclude the

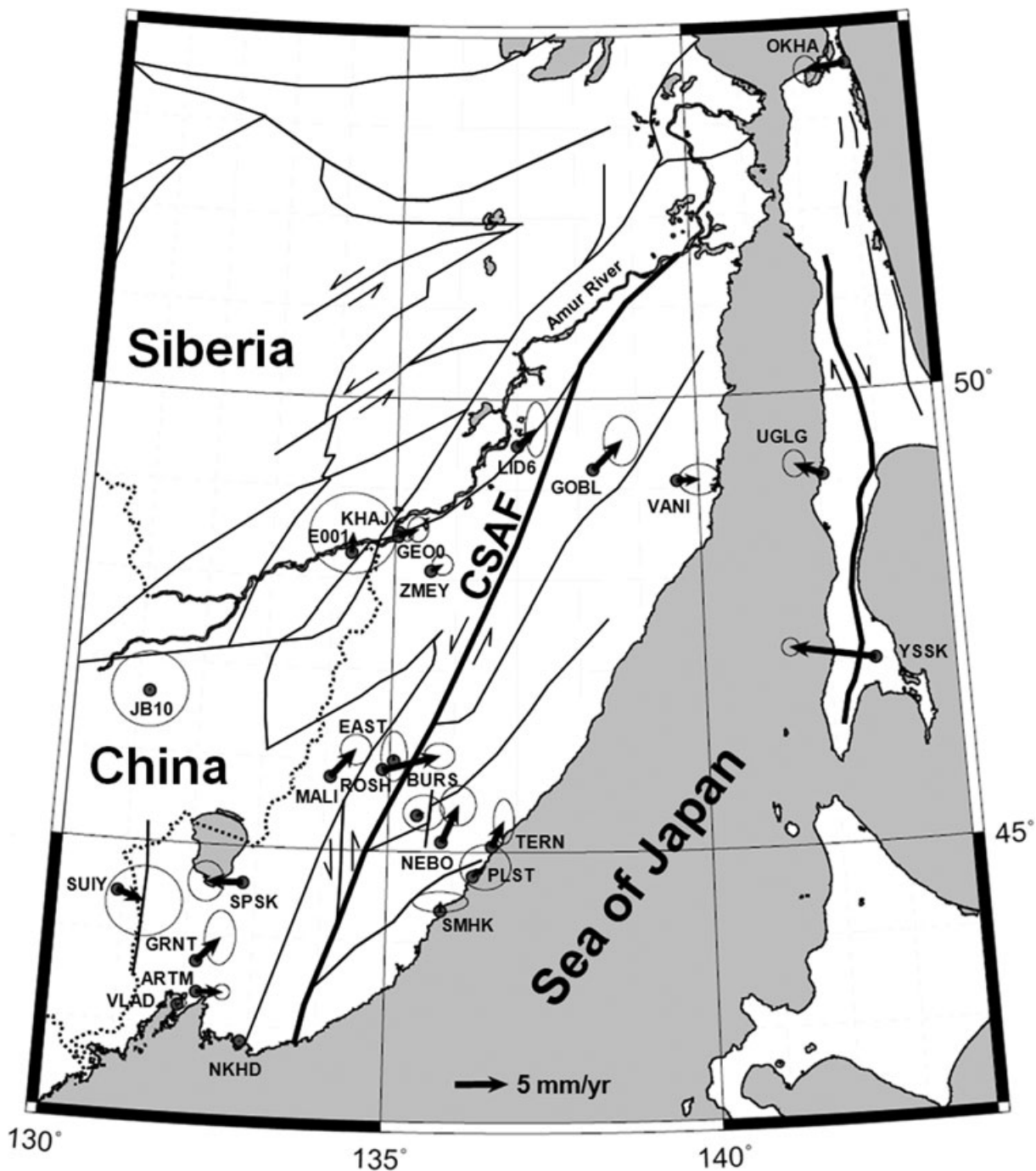


Figure 4. Horizontal GPS velocities referred to EUR. Error ellipses are 95% confidence. GPS velocities of the sites SUIY, JB10, E001 are calculated by using their ITRF2000 velocities taken from Meng *et al.* (2006) and are transformed into ITRF2008. Main faults are marked by solid and thin black lines. Arrows demonstrate relative slip directions along fault traces. The boundary between Russia and China is denoted by dotted line.

possibility of low-scale geodynamic activity associated with small independently moving crustal blocks and/or present-day activity of minor faults.

3.3 Obtained GPS velocity field and AMU microplate rigid rotation

In the continental part our GPS network stations are located not far from the northeastern boundary of the assumed AMU microplate (Zonenshain & Savostin 1981). The obtained velocity field confirms

almost absence of significant relative movements within the area under study. The EUR-velocities of all the stations are also small enough. Nonetheless, we verified how well the obtained velocity field corresponds to the conception of a separate rigid rotation of the AMU microplate with respect to EUR. The velocities of three Chinese GPS sites located near the investigated region were taken from Meng *et al.* (2006) and transformed into ITRF2008, referred to EUR as described in chapter 2, and were also combined with our GPS velocity field. The misfit between our GPS velocity field and the velocities predicted by a number of different models of the

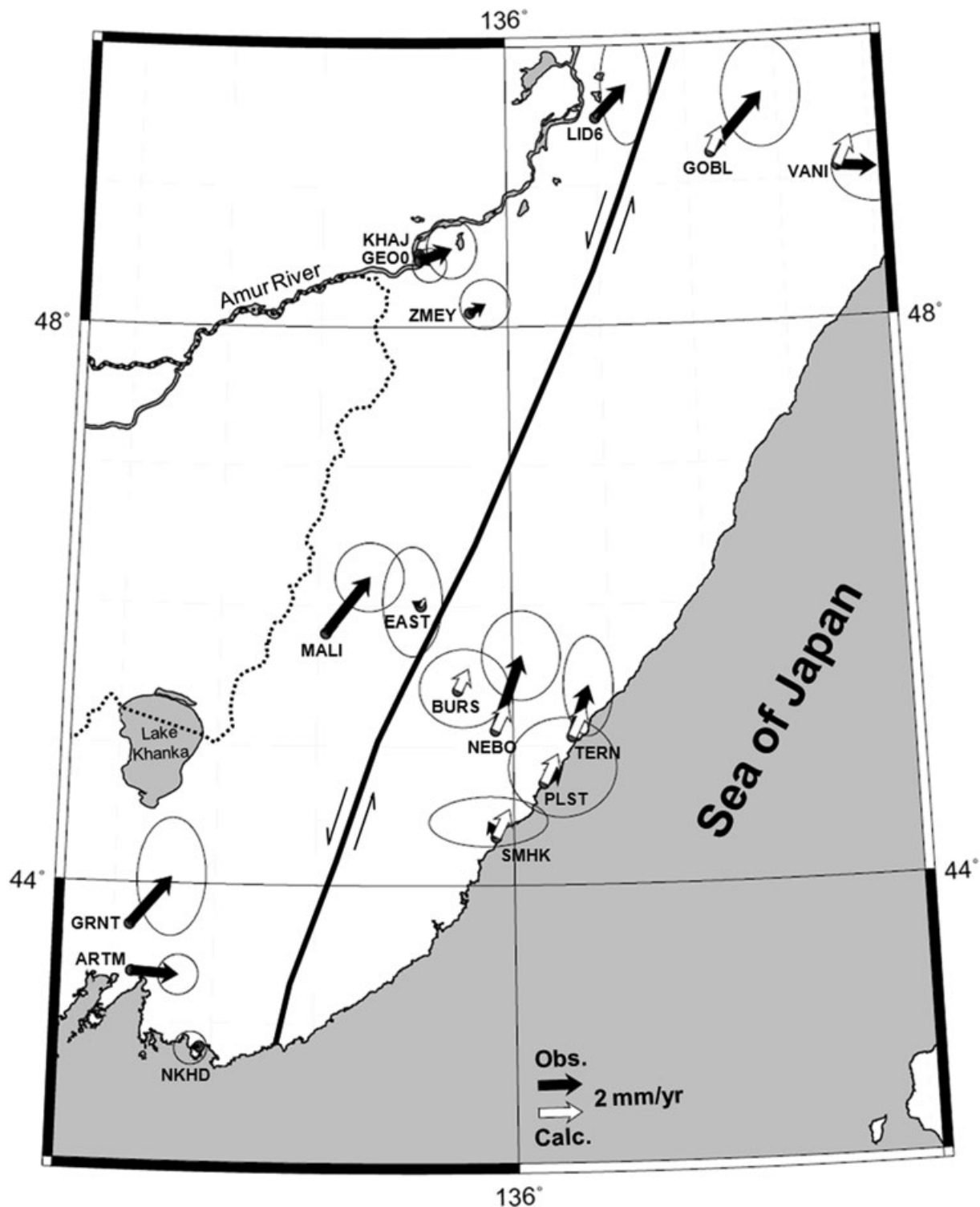


Figure 5. Horizontal velocities of network sites around the CSAF estimated from GPS observations and calculated by using an ideal left-lateral strike-slip locked fault model ($H = 40$ km and $V_H = 1.8$ mm yr $^{-1}$). All the velocities are referred to the VLAD site. The CSAF trace is denoted by solid black line.

AMU/EUR rigid rotation was estimated in terms of χ^2 assuming that the continental part of the area under study is located within the AMU stable interiors. A number of the AMU/EUR rotation models as large as 16 were tested and velocities of 20 GPS sites were used.

The obtained χ^2/df -values vary from 10 for the best-fit model to 527 for the worst-fit one, accordingly, for all the models. Taking into account these results and comparing the calculated and

observed velocity field for the tested AMU/EUR models one can subdivide them into a few groups. The models characterizing the appropriate groups are listed in Table 3 and shown in Fig. 6. The first group comprises the models developed by Heki *et al.* (1999), Holt *et al.* (2000), Calais *et al.* (2003) and Sella *et al.* (2002). These models are characterized by the highest misfit to the observed GPS velocities (χ^2/df -value changes from 59 to 527) and predict too

Table 3. AMU/EUR rotation poles taken from different models characterizing the appropriate model groups and appropriate χ^2/df -values calculated from comparison of the observed and model-predicted GPS site velocities.

No. of model group	No. of model	Models characterizing the appropriate model groups	AMU/EUR rotation pole parameters			Statistics		
			φ°	λ°	ω°/Myr	χ^2	df	χ^2/df
1	1	Heki <i>et al.</i> 1999	-22.30	106.60	-0.091	8962	17	527
2	2	Prawirodirdjo & Bock 2004	45.43	154.75	0.093	1144	17	67
3	3	England & Molnar 2005	64.80	156.10	0.060	603	17	35
	4	Meng <i>et al.</i> 2006	54.06	135.87	0.099	294	17	17
4	5	Wei & Seno 1998	60.42	123.25	0.025	170	17	10
5	6	Absence of AMU/EUR relative rotation, zero-velocity field	-	-	-	278	20	14

long northeast and southeast velocity vectors (Fig. 6a). The second group should include at least three models developed by Altamimi *et al.* (2007), Prawirodirdjo & Bock (2004) and Kreemer *et al.* (2006). The models of Sella *et al.* (2002) and Jin *et al.* (2007) can also be included into this group. The corresponding χ^2/df -values range from 28 to 67 for the best- and worst-fit models, respectively. This model group does not also demonstrate a qualitative agreement with our GPS velocity field mainly because all the models produce GPS velocities with domination of the south component. This result contradicts our estimates (Fig. 6a). The next set of the AMU/EUR models includes the models of Zonenshain & Savostin (1981), England & Molnar (2005), Timofeev *et al.* (2008), Kreemer *et al.* (2003), Apel *et al.* (2006), Calais *et al.* (2006), Meng *et al.* (2006) and is characterized by the misfit values ranging from 16 to 36. These models predict almost east and southeast velocities with the magnitudes in general more consistent with our estimates compared to previous groups. The model velocity magnitudes increase from north to south. However, our GPS velocity field does not show such a regular behaviour (see Figs 4, 6b). It is necessary to point out that some considered AMU/EUR models predicting small-magnitude velocity vectors are characterized by the relatively small misfit values despite qualitative disagreement with the observed GPS velocities. Finally, we found out that the best-fit model characterized by the smallest χ^2/df -value equal to 10 (Table 3) was developed by Wei & Seno (1998). It predicts very small northeast velocity vectors with the magnitudes less than 1 mm yr^{-1} and domination of the east component (see Fig. 6c). According to this, we additionally tested the zero-velocity field model (model 6 in Table 3), which implies the absence of rigid rotation of the AMU microplate with respect to EUR. The resulting χ^2/df -value is close enough to such an estimate for the best-fit model. These results lead us to the conclusion about almost stability or small relative movement of the southeast of Russia with respect to EUR. Moreover, if we reduce the rotation rate for all the tested models up to 0.02° per Myr, then χ^2/df -values for most calculated models will also reduce dramatically and will be close to this value for the best-fit model. This effect is quite obvious if the observed GPS velocities are small and comparable to their errors. In this case, location of the rotation pole is not so important and can be changed broadly whereas the rotation rate most significantly contributes to the predicted site velocities. Of course, such adjustment of the AMU/EUR rotation rate leads to significant discrepancies with the observed GPS velocities in the west (Calais *et al.* 2003; Calais *et al.* 2006; Wang *et al.* 2008) and southeast of the AMU microplate (Jin & Park 2006; Jin *et al.* 2007). In this case, perhaps, the AMU microplate could not be considered an indivisible rigid plate but rather a set of a few separately rotated blocks to one of which our continental GPS network would probably belong. To verify this assumption, the currently operating

continental GPS network should be expanded northward through the south of the Russian Far East and densified. Some evidences in favour of separate rotation of a number of crustal blocks in Northeast Asia have already been reported by Jin & Park (2006) and Jin *et al.* (2007).

4 CONCLUSIONS

The regional GPS network established during 1995–2009 expands the geodynamic GPS observations eastward and northeastward from Northeast China thus partially filling in the gap in geodetic measurements, which exists in the Far East of Russia (Eastern Siberia).

The obtained velocity field confirms that the continental part of the southeast of Russia belongs to the EUR plate whereas Sakhalin Island can be associated with the NAM plate or the OKH microplate.

The calculated GPS velocities indicate almost internal (between network sites) and external (with respect to EUR) stability of the investigated region with a local manifestation of notable geodynamic activity which may be associated with the movement of small independent crustal blocks and/or present-day tectonic activity of minor faults or other tectonic structures.

We have not found clear evidences of any significant present-day tectonic activity of the CSAF as a whole. The obtained GPS velocity field indicates a small eastward movement (almost stability) of the southeast of Russia with respect to EUR. This may indicate the existence of a few separate blocks and testify to a more sophisticated structure of the proposed AMU microplate in comparison with an indivisible plate approach. The future expanding of the currently operating GPS network northward through Eastern Siberia can provide us with the data to verify this assumption.

ACKNOWLEDGMENTS

The first author thanks the Institute of Seismology and Volcanology (ISV), Sapporo, Japan for the opportunity to do this research during his stay in ISV as visiting associate professor. We would like to thank Mikhail Kogan and Dr Meng Guojie for their valuable comments and help in the GPS solutions comparison. Authors are grateful to prof. Duncan Agnew, prof. Kosuke Heki and anonymous reviewer for their helpful and constructive remarks about this manuscript. We would like to thank all the people who helped us to carry out semi-continuous and survey-mode GPS observations in Primorye and the Khabarovsk Krai. This work was supported by the grant of the President of the Russian Federation for young scientists MK-4573.2009.5, by the grants of FEB RAS No.

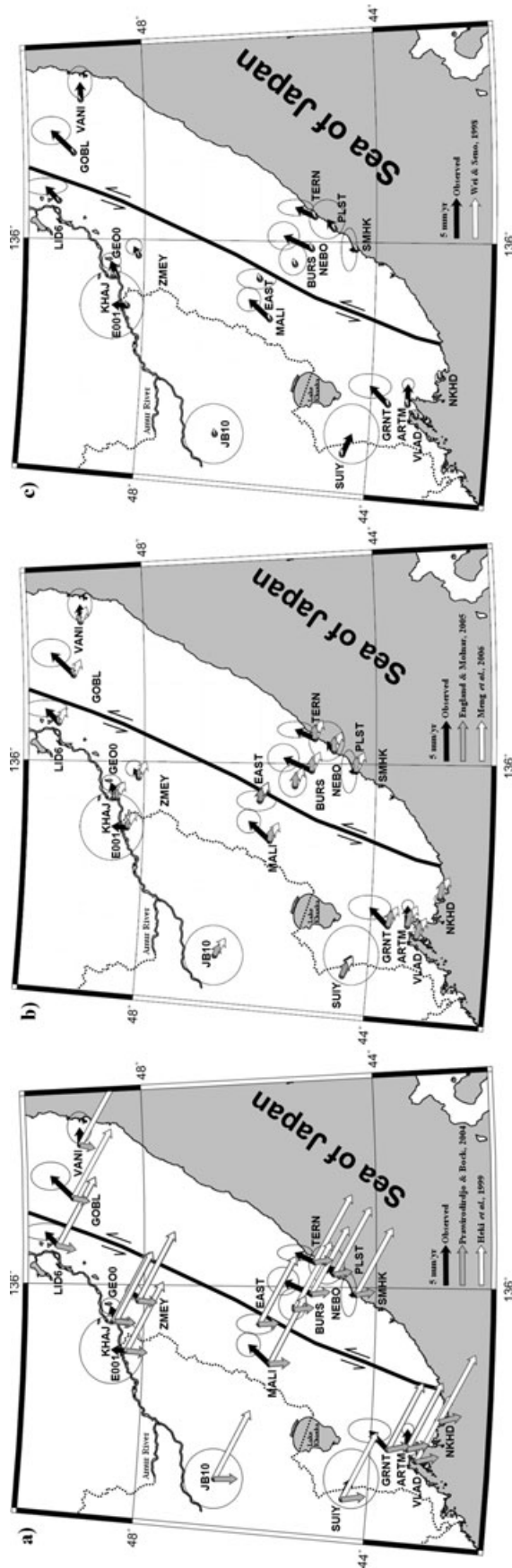


Figure 6. Horizontal velocities of the southeast of Russia estimated from GPS observations and calculated by using different AMU/EUR rigid rotation models characterizing the appropriate model groups: (a) Hehl *et al.* 1999 (first group), Prawirodirdjo & Bock 2004 (second group); (b) England & Molnar 2005 and Meng *et al.* 2006 (third group); (c) Wei & Seno 1998 (fourth group). All the velocities are referred to EUR. The CSAF trace is denoted by solid black line.

09-III-A-08-441, 10-III-B-08-025 and by the Program of Fundamental Researches of FEB RAS 'Recent geodynamics, active geologic structures and natural hazards of the Russian Far East'. Our study was also supported by Grant-in-Aid for Scientific Research (KAKENHI, A-21253005) and Observation and Research Program for Prediction of Earthquakes and Volcanic Eruptions from the Ministry of Education, Culture, Sports, Science and Technology (MEXT) of Japan. The GMT software (Wessel & Smith 1998) was partially used to plot figures. The Fortran-77 code developed by Kosuke Heki was used for the absolute rotation poles calculation.

REFERENCES

- Altamimi, Z., Collilieux, X., Legrand, J., Garayt, B. & Boucher, C., 2007. ITRF2005: a new release of the International Terrestrial Reference Frame based on time series of station positions and Earth Orientation Parameters, *J. geophys. Res.*, **112**, B09401, doi:10.1029/2007JB004949.
- Altamimi, Z., Sillard, P. & Boucher, C., 2002. ITRF2000: a new release of the International Terrestrial Reference Frame for earth science applications, *J. geophys. Res.*, **107**(B10), 2214, doi:10.1029/2001JB000561.
- Apel, E.V., Bürgmann, R., Steblov, G., Vasilenko, N., King, R. & Pritchard, A., 2006. Independent active microplate tectonics of northeast Asia from GPS velocities and block modeling, *Geophys. Res. Lett.*, **33**, L11303, doi:10.1029/2006GL026077.
- Argentov, V.V., Gnibidenko, G.S., Popov, A.A. & Potap'ev S.V. 1976. *The Deep Structure of Primorye*, Nauka, Moscow. (in Russian)
- Argus, D.F. & Gordon, R.G., 1991. No-net-rotation model of current plate velocities incorporating plate motion model NUVEL-1, *Geophys. Res. Lett.*, **18**(11), 2039–2042, doi:10.1029/91GL01532.
- Beutler, G. et al. 2007. Bernese GPS software version 5.0, Astron. Inst., Univ. of Bern, Bern, Switzerland.
- Brockmann, E., 1997. Combination of Solutions for Geodetic and Geodynamic Applications of the Global Positioning System (GPS), *Geodätisch-geophysikalische Arbeiten in der Schweiz*, Band 55, Schweizerische Geodätische Kommission, Institut für Geodäsie und Photogrammetrie, Eid. Technische Hochschule Zürich, Zürich.
- Bürgmann, R., Kogan, M., Steblov, G., Hillel, G., Levin, V. & Apel, E., 2005. Interseismic coupling and asperity distribution along the Kamchatka subduction zone, *J. geophys. Res.*, **110**, B07405, doi:10.1029/2005JB003648.
- Calais, E., Dong, L., Wang, M., Shen, Z. K. & Vergnolle, M., 2006. Continental deformation in Asia from a combined GPS solution, *Geophys. Res. Lett.*, **33**, L24319, doi:10.1029/2006GL028433.
- Calais, E., Vergnolle, M., San'kov, V., Likhnev, A., Miroshnichenko, A., Amarjargal, S. & De'verche're, J., 2003. GPS measurements of crustal deformation in the Baikal-Mongolia area (1994–2002): Implications for current kinematics of Asia, *J. geophys. Res.*, **108**(B10), 2501, doi:10.1029/2002JB002373.
- DeMets, C., Gordon, R.G., Argus, D.F. & Stein, S., 1994. Effect of recent revisions to the geomagnetic time scale on estimates of current plate motion, *Geophys. Res. Lett.*, **21**(20), 2191–2194, doi:10.1029/94GL02118.
- England, P. & Molnar, P., 2005. Late Quaternary to decadal velocity fields in Asia, *J. geophys. Res.*, **110**, B12401, doi:10.1029/2004JB003541.
- Geirsson, H. et al. 2006. Current plate movements across the Mid-Atlantic Ridge determined from 5 years of continuous GPS measurements in Iceland, *J. geophys. Res.*, **111**, B09407, doi:10.1029/2005JB003717.
- Gordeev, E., Gusev, A.A., Levin, V.E., Bakhtiarov, V.F., Pavlov, V.M., Chebrov, V.N. & Kasahara, M., 2001. Preliminary analysis of deformation at the Eurasia-Pacific-North America plate junction from GPS data, *Geophys. J. Int.*, **147**, 189–198, doi:10.1046/j.0956-540x.2001.01515.x
- Heki, K. et al. 1999. The Amurian Plate motion and current plate kinematics in eastern Asia, *J. geophys. Res.*, **104**(B12), 29147–29155.
- Holt, W.E., Chamot-Rooke, N., Pichon, X. Le, Haines, A.J., Shen-Tu, B. & Ren, J., 2000. Velocity field in Asia inferred from Quaternary fault slip rates and Global Positioning System observations, *J. geophys. Res.*, **105**(B8), 19185–19209.
- Ivanov, B.A., 1972. *The Central Sikhote-Alinsky Fault*, Dalnauka, Vladivostok. (in Russian)
- Jin, S. & Park, P.H., 2006. Does the Southern Korean Peninsula belong to the Amurian plate? GPS observations, *Studia Geophysica et Geodaetica*, **50**(4), 633–644, doi:10.1007/s11200-006-0040-x.
- Jin, S., Park, P. & Zhu, W., 2007. Micro-plate tectonics and kinematics in Northeast Asia inferred from a dense set of GPS observations, *Earth planet. Sci. Lett.*, **257**, 486–496.
- Karsakov, L.P. et al. 2001. *Tectonic Map of the Central Asian-Pacific Belts Junction Area Transition Zone (scale 1:1500000)*, Khabarovsk-Shenyang, ITG FEB RAS, Khabarovsk.
- Kato, T., 2003. Tectonics of the eastern Asia and the western Pacific as seen by GPS observations, *Geosci. J.*, **7**(1), 1–8.
- Kato, T. et al. 1998. Initial Results from WING, the Continuous GPS Network in the Western Pacific Area, *Geophys. Res. Lett.*, **25**(3), 369–372.
- Kogan, M.G. & Steblov, G.M., 2008. Current global plate kinematics from GPS (1995–2007) with the plate-consistent reference frame, *J. geophys. Res.*, **113**, B04416, doi:10.1029/2007JB005353.
- Kogan, M.G. et al. 2000. Geodetic constraints on the relative motion and rigidity of Eurasia and North America, *Geophys. Res. Lett.*, **27**(14), 2041–2044, doi:10.1029/2000GL011422.
- Kogan, M.G. et al. 2003. The 2000 Mw 6.8 Uglegorsk earthquake and regional plate boundary deformation of Sakhalin from geodetic data, *Geophys. Res. Lett.*, **30**(3), 1102, doi:10.1029/2002GL016399.
- Kreemer, C., Holt, W.E. & Haines, A.J., 2003. An integrated global model of present-day plate motions and plate boundary deformation, *Geophys. J. Int.*, **154**, 8–4.
- Kreemer, C., Laval'e, D.A., Blewitt, G. & Holt, W.E., 2006. On the stability of a geodetic no-net-rotation frame and its implication for the International Terrestrial Reference Frame, *Geophys. Res. Lett.*, **33**, L17306, doi:10.1029/2006GL027058.
- Lisowski, M., Savage, J.C. & Prescott, W.H., 1991. The Velocity Field Along the San Andreas Fault in Central and Southern California, *J. geophys. Res.*, **96**(B5), 8369–8389.
- Mazzotti, S., Pichon, X.Le., Henry, P. & Miyazaki, S., 2000. Full interseismic locking of the Nankai and Japan-west Kurile subduction zones: an analysis of uniform elastic strain accumulation in Japan constrained by permanent GPS, *J. geophys. Res.*, **105**(B6), 13159–13177.
- Meng, G., Shen, X., Wu, J. & Rogozhin, E.A., 2006. Present-day crustal motion in northeast China determined from GPS measurements, *Earth Planets Space*, **58**, 1441–1445.
- Nazarenko L. & Bazhanov, V.A., 1987. *Geology of Primorsky Krai. Part III. Main Tectonic Settings and Evolution History*. Preprint, Vladivostok. (in Russian)
- Oleynikov, A.V. & Oleynikov, N.A., 2006. Paleoseismogeology and seismic hazard in Primorye, *Vestn. FEB RAS*, **3**, 76–84. (in Russian)
- Prawirodirdjo, L. & Bock, Y., 2004. Instantaneous global plate motion model from 12 years of continuous GPS observations, *J. geophys. Res.*, **109**, B08405, doi:10.1029/2003JB002944.
- Sella, G.F., Dixon, T.H. & Mao, A., 2002. REVEL: A model for recent plate velocities from space geodesy, *J. geophys. Res.*, **107**(B4), 2081, doi:10.1029/2000JB000033.
- Seno, T., Sakurai, T. & Stein, S., 1996. Can the Okhotsk plate be discriminated from the North American plate?, *J. geophys. Res.*, **101**, 11305–11315, doi:10.1029/96JB00532.
- Steblov, G.M., Kogan, M.G., King, R.W., Scholz, C.H., Bürgmann, R. & Frolov, D.I., 2003. Imprint of the North American plate in Siberia revealed by GPS, *Geophys. Res. Lett.*, **30**(18), 1924, doi:10.1029/2003GL017805.
- Stein, S. & Gordon, R.G., 1984. Statistical tests of additional plate boundaries from plate motion inversions, *Earth planet. Sci. Lett.*, **69**(2), 401–412.
- Takahashi, H. et al. 1999. Velocity field of around the Sea of Okhotsk and sea of Japan regions determined from a New Continuous GPS Network Data, *Geophys. Res. Lett.*, **26**(16), 2533–2536.
- Timofeev, V.Yu., Gornov, P.Yu., Ardukov, D.G., Malyshev, Yu.F. & Boiko E.V., 2008. GPS measurements (2003–2006) in the Sikhote Alin network, the Far East, *Russ. J. Pac. Geol.*, **2**(4), 314–324, doi:10.1134/S1819714008040040.

- Toya, Y. & Kasahara, M., 2005. Robust and exploratory analysis of active mesoscale tectonic zones in Japan utilizing the nationwide GPS array, *Tectonophysics*, **400**(1–4), 27–53.
- Wang, J., Ye, Z-R. & He, J-K., 2008. Three-dimensional mechanical modeling of large-scale crustal deformation in China constrained by the GPS velocity field, *Tectonophysics*, **446**, 51–60.
- Wang, Q., et al. 2001. Present-day crustal deformation in China constrained by Global Positioning System measurements, *Science*, **294**, 574–577.
- Wei, D. & Seno, T., 1998. Determination of the Amurian plate motion, in *Mantle Dynamics and Plate Interactions in East Asia*, in *Geodyn. Ser.*, **27**, pp. 337–346, ed. Flower, M.F.J. et al. AGU, Washington, D.C..
- Wessel, P. & Smith, W.H.F., 1998. New, improved version of Generic Mapping Tools released, *Eos Trans. AGU*, **79**, 579, doi:10.1029/98EO00426.
- Zonenshain, L.P. & Savostin, L.A., 1981. Geodynamics of the Baikal rift zone and plate tectonics of Asia, *Tectonophysics*, **76**, 1–45, doi:10.1016/0040-1951(81)90251-1.